# Monte Carlo simulation of the role of defects as a melting mechanism

L. Gómez,[1,2] A. Dobry,[1,2] and H. T. Diep[1]

[1]*Departamento de Física, Universidad Nacional de Rosario and Instituto de Física Rosario, Avenida Pellegrini 250, 2000 Rosario, Argentina*

[2]*Laboratoire de Physique Théorique et Modélisation, Université de Cergy-Pontoise, 5, mail Gay-Lussac, Neuville sur Oise, 95031 Cergy-Pontoise Cedex, France*

(Received 21 June 2000; revised manuscript received 26 December 2000; published 8 May 2001)

We study in this paper the melting transition of a crystal of a fcc structure with the Lennard-Jones potential, by using isobaric-isothermal Monte Carlo simulations. Local and collective updates are sequentially used to optimize the convergence. We show the important role played by defects in the melting mechanism in favor of modern melting theories.

DOI: 10.1103/PhysRevB.63.224103 PACS number(s): 64.60.Cn, 05.70.Fh, 75.10.−b

## I. INTRODUCTION

The melting of crystals has always been an exciting subject in condensed matter physics.[1,2] The Lindemann criterion allows us to estimate the melting temperature in a simple way. However, the mechanism responsible for the melting is still debated. It was widely admitted that the melting in three dimensions (3D) occurs when one of the phonon modes is softened by the temperature $T$ so that instability of the crystalline phase takes place leading to the liquid phase. In 2D, this scenario is not valid. Mermin[3] has shown in 1968 that long-range crystalline order is destroyed by $T$ if the elastic interaction is power-law decayed with distance. Nelson and Halperin[4] have shown that the 2D melting is due to defects, analogous to the case of Kosterlitz-Thouless transition for $XY$ spins in 2D.[5,6] Inspired by this defect-mediated melting, several workers have attempted to prove that in 3D the melting may also be due to dislocations and defects.[7–12] The soft-mode scenario, though theoretically possible, is not the one frequently observed in numerical calculations. Works on defect theory up to 1989 have been summarized and developed in the book by Kleinert.[7] Recently, several numerical investigations[8–10] and analytic approximations[11,12] have shown that dislocations and defects are responsible for melting. In particular, Burakowsky, Prestoni, and Silbar[12] have shown that melting properties of most of elements of the Periodic Table can be explained by excitations of linear dislocations in the crystal using a polymer theory.

Katsnelson and Trefilov[11] have also recently developed a route toward a melting theory based in defects. They have emphasized the concept of the geometrical frustration,[13] i.e., the 3D Euclidean space cannot be filled by the closest packing structure, the tetrahedral one. Therefore they proposed that superdense regions and voids around them are to be formed near melting by thermal activation. These regions were suggested to be the precursor of the destruction of the crystalline order.

In this paper, we investigate by Monte Carlo (MC) simulation the melting of a 3D crystal where atoms interact with each other via the Lennard-Jones (LJ) potential. We show that defects which occur in the solid phase when the transition temperature is approached from below are responsible for the melting. Section II is devoted to a description of our model and MC method. Results are shown in Sec. III. Concluding remarks are given in Sec. IV.

## II. MODEL AND MONTE CARLO METHOD

We consider a crystal of face-centered cubic (fcc) structure which is described by the following Hamiltonian

$$\mathcal{H}=\sum_{(ij)} U(r_{ij}), \tag{1}$$

where the interaction between atoms at $r_i$ and $r_j$ is described by the potential $U(r_{ij})$. For simplicity, the distance dependence is supposed to be given by the LJ potential $U(r_{ij}) = 4\epsilon[(r_0/r_{ij})^{12}-(r_0/r_{ij})^6]$, where $r_{ij}=r_i-r_j$, $r_0$, being a characteristic length of the system, is chosen in such a way that the nearest-neighbor (NN) distance in the fcc lattice is equal to $\sqrt{2}/2$ when only NN interactions are taken into account. The fcc lattice constant is therefore equal to 1 in the ground state. Different potentials for cohesive interactions are possible, for example the so-called Gupta many-body potential[14] which has been recently used to study the melting process of a fcc crystal.[10] We have shown that defects created near melting play an important role in the melting mechanism. In the present paper we would like to clarify how defects are topologically distributed and how they destroy the crystal order. To this end, we choose the LJ potential which is simpler for implementing a volume-variable algorithm as will be described below. However, most of the conclusions concerning the melting mechanism are similar for these two potentials. Details of a precise comparison will be given elsewhere.

In this work, we studied a fcc lattice with different system sizes, using periodic boundary conditions, at constant pressure. Interactions up to a cutoff distance $r_c=1.57$ have been taken into account. This is about the fourth-nearest-neighbor distance in the perfect fcc crystal.

The following algorithm was used. Starting from the solid state where atoms are on the fcc lattice sites, we heat the system up to a temperature $T$. We equilibrate the system first locally at constant volume and then globally at variable volume, as explained hereafter. The local equilibration at constant volume is done as follows: we take an atom and move

 

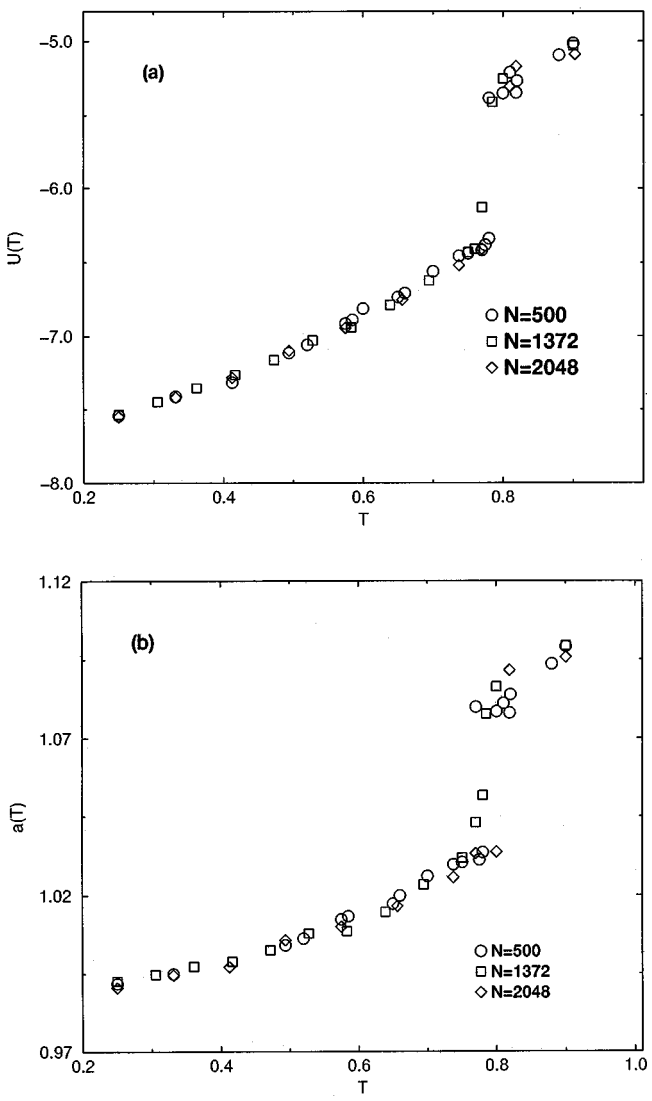


FIG. 1. (a) Internal energy $U$ vs $T$. (b) Lattice constant vs $T$ for the system of $N=1372$. The jumps at the transition temperature indicate the first-order character.

it to a nearby random position. This position is accepted if it lowers the atom energy. Otherwise it is accepted with a probability according to the Metropolis algorithm. We repeat this for all atoms: we say we achieve one MC step/atom. Next, we change the system volume by a random amount: all atom positions are thus rescaled with the volume variation. We recalculate the energy and accept or reject this volume using a constant pressure Metropolis algorithm. For a general method, see Ref. 15. In the following we work at zero pressure. We find that the equilibrium is reached very fast with alternately 10 consecutive local MC steps/atom followed by one volume variation step, and so forth. In all, we performed about $10^5$ MC sweepings at each $T$. Physical quantities such as averaged internal energy per atom $U$ and radial distribution function $g(r)$ are averaged over the next $10^5$ MC steps/atom.

From the plot of $\langle E \rangle$ versus $T$, we can identify the transition temperature from solid to liquid state. Furthermore, to investigate the melting mechanism we have computed the

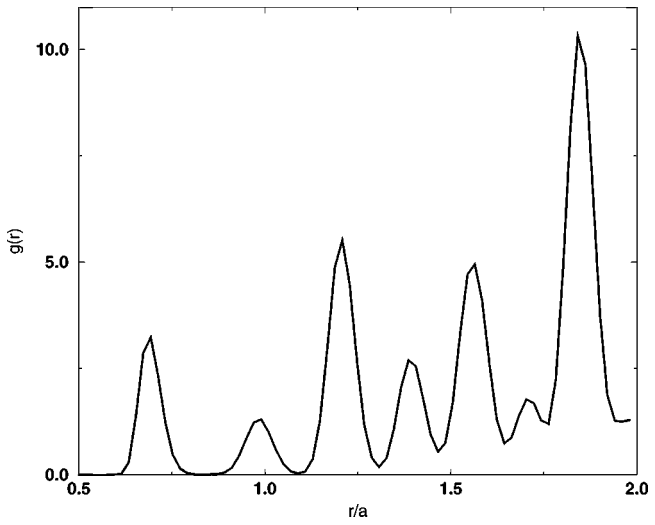


FIG. 2. Radial distribution function $g(r)$ at $T=0.25$. This function gives the mean value of the number of particles sitting at distance $r$ from a given particle.

following quantities: angular distribution of neighbors, distribution of defects, number of nearest-neighbors (NN), etc. As we discuss below, due to the particular fcc structure we cannot use the Voronoi method which would give confusing results if care is not taken.

## III. RESULTS

Let us show first in Fig. 1(a) $U$ versus $T$. One observes a discontinuity of $U$ indicating clearly that the transition is of first-order as expected for a 3D melting. This is confirmed by the jump of the average fcc lattice constant shown in Fig. 1(b). These figures show results for three different system sizes. Since the transition is of first order, the transition temperature $T_m$ cannot be defined with precision (due to hysteresis). Moreover, for sizes greater than 500 particles the melting temperatures fall within the same interval. Therefore, in the following we will show results for the system of $N=1372$ particles. We take $T_m$ as the lower limit of the transition temperature region. From Fig. 1, we take $T_m=0.76$. Note that as our simulation cell does not contain surfaces, this transition temperature corresponds to the metastability limit of the crystal's ability to superheat rather than to the thermodynamical melting point.[16,17] In the following, we will call for simplicity, $T_m$ at this transition temperature and associate the phenomena with an apparent melting point since the structure losses all local order at this temperature.

Figure 2 shows the radial distribution function between atoms at a low $T$ ($T=0.25$) in the solid phase. The first (second, third, . . . ) peak corresponds to the NN (NNN, third neighbors, . . . ) distance of the fcc structure.

To calculate the coordination number $c$ of a site, we integrate the radial distribution function up to the first minimum. For example in Fig. 2, integrating $g(r)$ over $r$ up to about $r_1=0.85$ (first minimum) will give $c=12$. Integrating $g(r)$ from $r_1$ up to the next minimum at $r_2=1.1$ gives $c_2=6$, and so on. These coordination numbers verify the fcc structure. We use this method instead of the frequently used Voronoi

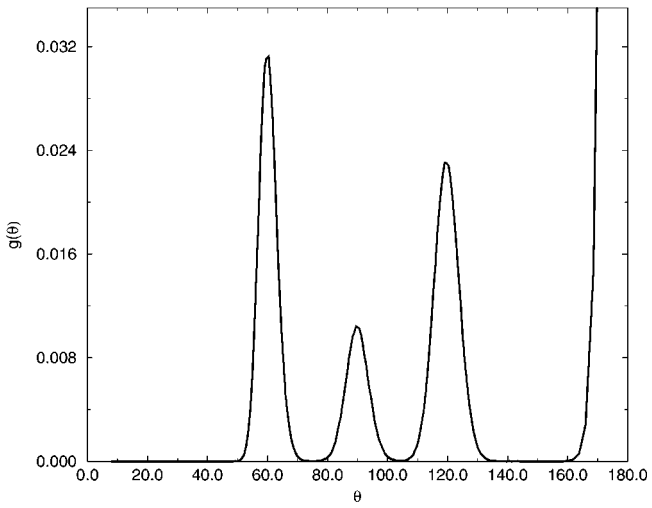


FIG. 3. Angular distribution function as defined in the text at $T=0.25$. The area below $g(\theta)$ is normalized to one.

construction because the Voronoi polyhedra in a slightly distorted fcc structure have small faces and short edges and the coordination number could not be precisely calculated because these small faces appear and disappear frequently due to thermal excitations.[9,18]

Furthermore, to complete our structure determination, we also calculate $g(\theta)$, the angular distribution of neighbors around a site within a plane up to a certain distance. The function $g(\theta)$ gives the probability to have two neighbors of an atom forming an angle $\theta$. We show in Fig. 3 an example of angular distribution taken at $T=0.25$ . The peak at 60 (90, 120) degrees corresponds to the angular distribution of the NN (NNN, 3rd NN) atoms in the fcc structure.

Let us increase $T$ near the transition. The radial distribution $g(r)$ at $T=0.7$ is shown in Fig. 4. The main differences with the low-$T$ structure shown in Fig. 2 are:

- All the minima between the peaks are raised. This is evidence that the crystal order is reduced at $T=0.7$. In particular, the minimum between the first and second peaks does not correspond to $g(r)=0$. This implies that a diffusional dynamics is activated near melting. This is the origin of the formation of defect clusters we will discuss below.
- Another feature is the strong reduction of the second and fourth peaks. The cubic symmetry is therefore weakened and the remaining correlated part of the system is within the (111) planes.

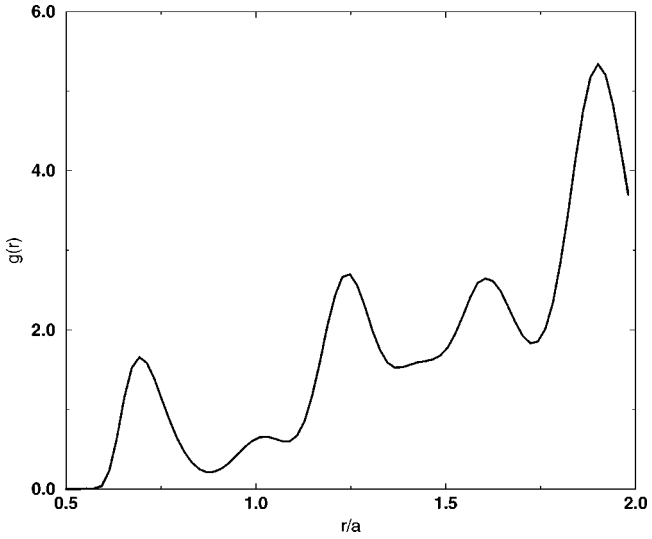


FIG. 4. Function $g(r)$ at $T=0.7$.

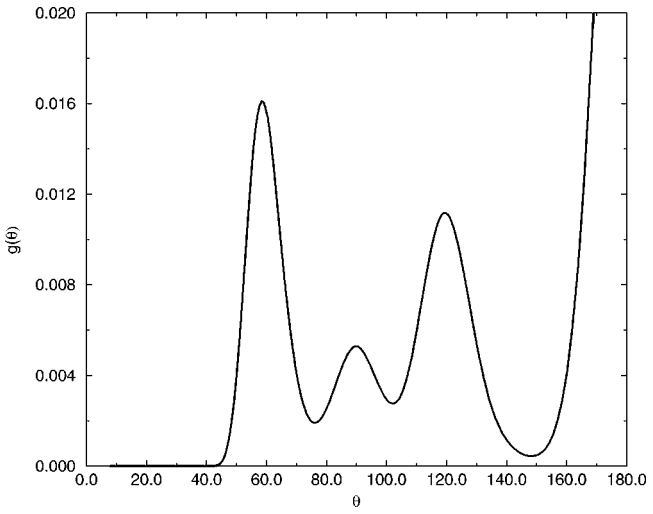


FIG. 5. Angular distribution function $g(\theta)$ at $T=0.7$.

Integrating $g(r)$ over $r$ between two consecutive minima, one obtains the coordination number $c=12$ only at 74% of the total crystal sites. 15.5% of the sites have 11 NN, 7.3% have 13 NN, and 2% have 10 NN. At this stage, it is worthwhile to stress that though the temperature is still below $T_m$, such an important percentage of sites (26%) exhibit defects. The crystal structure, therefore, cannot be considered as a defect-free one which is used in the search for a phonon soft-mode responsible for the elasticity instability at the melting.

The angular distribution for $T=0.7$ is shown in Fig. 5. One observes a strong deviation from the low-$T$ one shown in Fig. 3. The cubic symmetry is reduced and the persistence of the (111) structure is seen in this figure: the peak at 90°, characteristic of the cubic symmetry, is broadened and reduced whereas the other two peaks of the (111) one still have some structure.

For $T=0.79$, i.e., a temperature just above the transition, we find the following striking result: 30% of sites with 11 NN, 25% with 10 NN, 20% with 12 NN, 12% with 9 NN, 4% with 8 NN, 6% with 13 NN, 1% with 7 NN, and with 14 NN. Note that the percentage of 12 NN atoms has dropped from 74% at $T=0.7$ to 20% at this temperature. The average NN number is therefore 10.71.

Let us analyze now the structure of the observed defects. For this purpose we calculated the radial and angular distributions *between defects* as follows: whenever we are at a defect, i.e., atom with a coordination number different from 12, we search for defects around it up to a certain distance

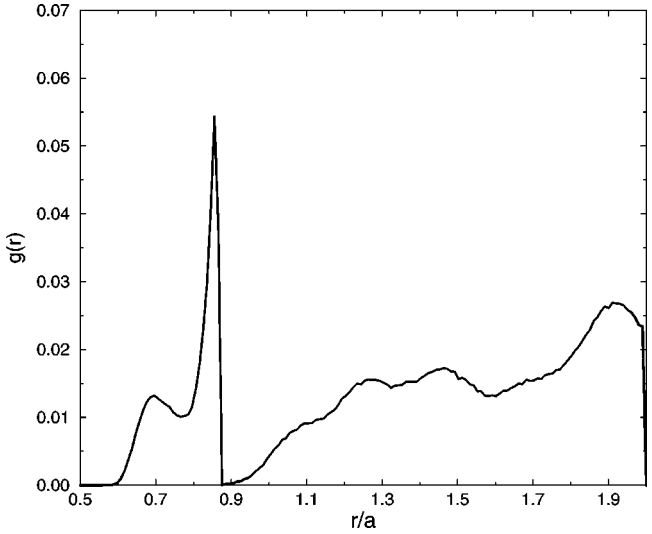


FIG. 6. Radial distribution function *between* defects of coordination $c=13$ at $T=0.7$. Note the different scale with Fig. 2 because we fixed the area below $g(r)$ to be one here.

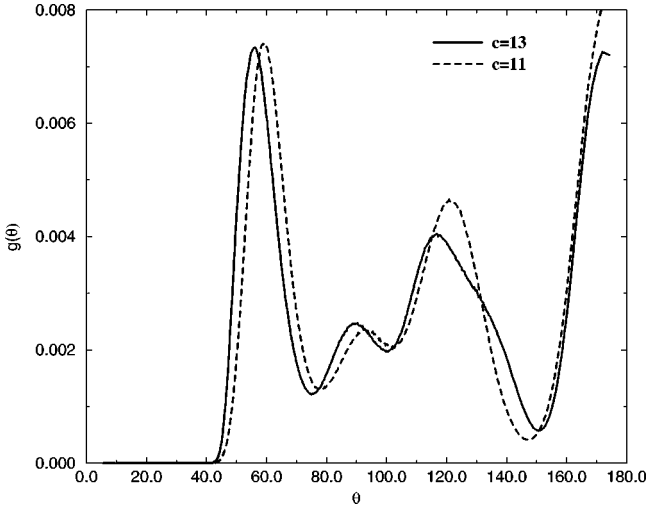


FIG. 8. Angular distribution around defects of coordination $c=11$ and 13 at $T=0.5$.

and realize histograms. Figure 6 shows the radial distribution of defects at $T=0.7$ around defects with $c=13$. One observes that (i) the defects are surrounded by other defects at a distance (0.696) slightly shorter than the equilibrium NN distance indicating that at this temperature defects form clusters and (ii) there is a larger number of defects at a distance 0.876 very close to $\sqrt{3}/2$, indicating that defects occupy the sites at the middle of the fcc cube which are normally vacant in the equilibrium configuration. This finding is important since it shows that defects forms clusters with two shells: the inner are defects at 0.696 and the outer at 0.876 from the center defect. At this temperature, these kinds of defects are uncorrelated at larger distances (see Fig. 6). The situation for defects with $c=11$ is shown in Fig. 7. In this case the second peak is less intensive and order at larger distances appears as we discuss below. Angular distributions between defects at $T=0.7$ show a shift of a few degrees of the peaks toward smaller angles for defects with $c=13$ as expected for $c$ larger than 12 (see Fig. 8). However, for defects with $c=11$, only the first peak is lowered, while the other two peaks are shifted a few degrees higher.

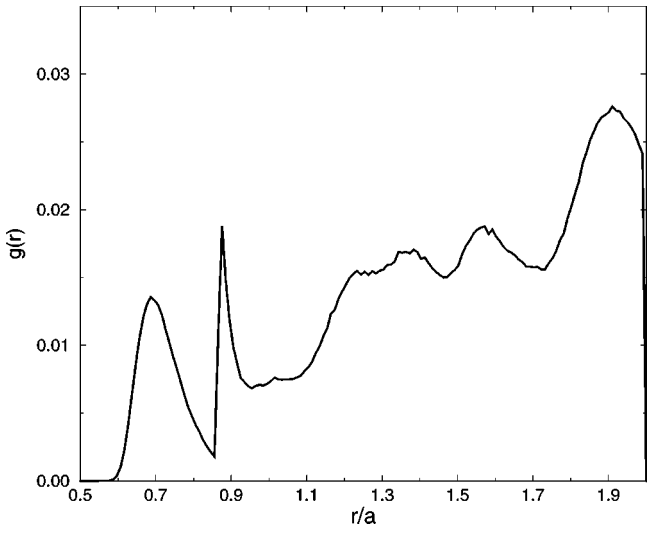


FIG. 7. The same as Fig. 6 but for defects with $c=11$.

Let us analyze more carefully the distribution of the clusters formed by the defects. We have computed the number of defects *inside* each cluster. As we previously stated we have seen that defects are not isolated but they are arranged in separated inner and outer groups within a defect cluster. The outer groups appear and disappear while the simulation evolves, making the cluster size vary. To quantify the sizes of these clusters we have obtained a histogram representing the probability to have a cluster with a given number of particles. The results are plotted in Fig. 9 at low, intermediate, and near melting point temperatures. At low temperature [Fig. 9(a)], where the density of defects is very low, they appear mainly in pairs. These pairs of defects are completely isolated and not important for the thermodynamical properties. As the temperature increases, larger clusters of defects start to be created [Fig. 9(b)]. Note that at temperatures near melting, clusters of all sizes are present with the same probability up to a large given number of particles [Fig. 9(c)]. When the cluster size reaches a given critical value the system melts. We can interpret these defect clusters as a set of dislocation arrays or alternatively as liquid zones inside a solid bulk. To enforce this interpretation we show the radial distribution between defects in Fig. 10 for defects with $c=13$ at $T=0.79$. One observes a large double peak indicating defects at distances between NN and NNN equilibrium distances and pronounced peaks at around 3rd neighbor distance ($\sqrt{2}$) and at 2. This suggests that defects are linked over large distances near the transition. Note that this correlation is in fact insinuated below $T_m$ as is seen in Fig. 7 for defects of $c=11$ at $T=0.7$. The scenario proposed by Burakowsky, Prestoni, and Silbar[12] is somewhat verified. We recall that this theory states that melting appears as a result of

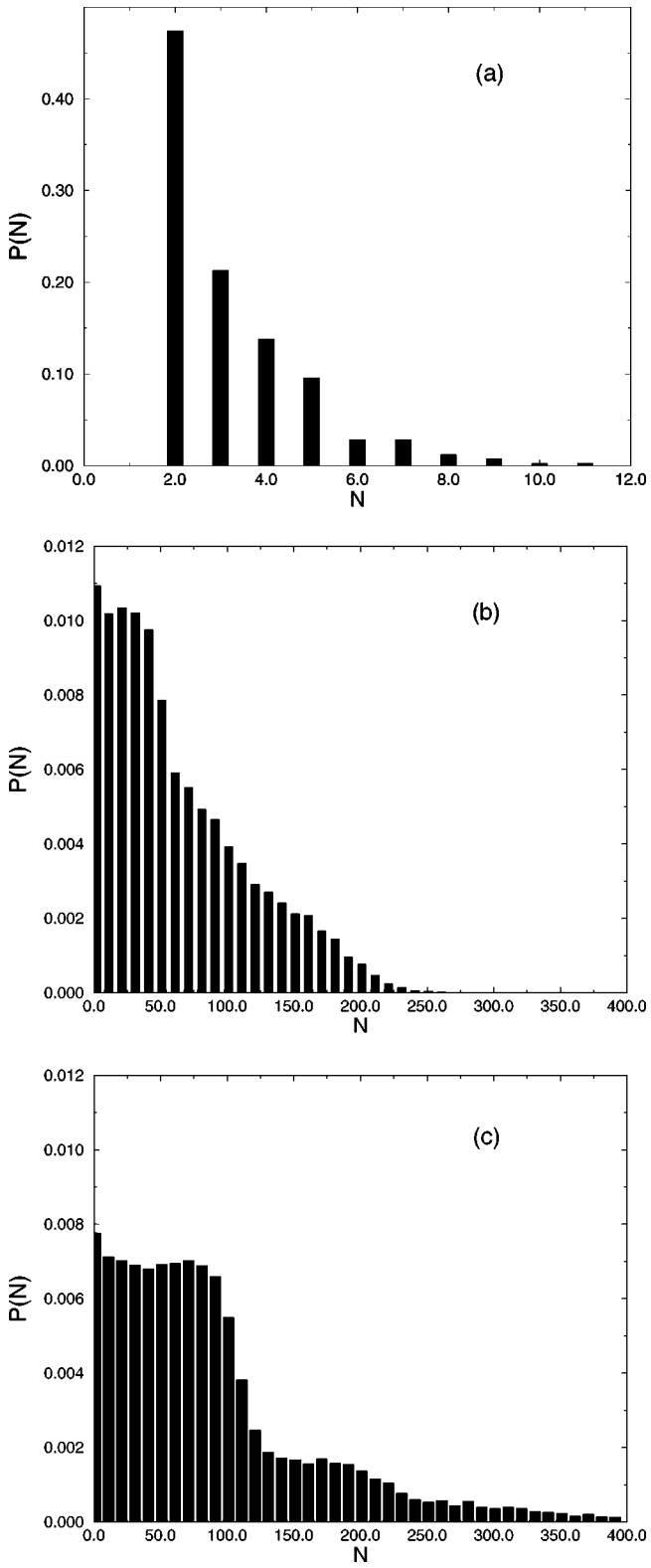


FIG. 9. Histogram of the number of defects in a cluster for (a) $T=0.3$, (b) $T=0.58$, and (c) $T=0.725$.

dislocation generation. When the density of the dislocation array reaches a given critical value, the entropy of these arrays compensates the increase of energy produced by the local breakdown of the perfect crystalline order.

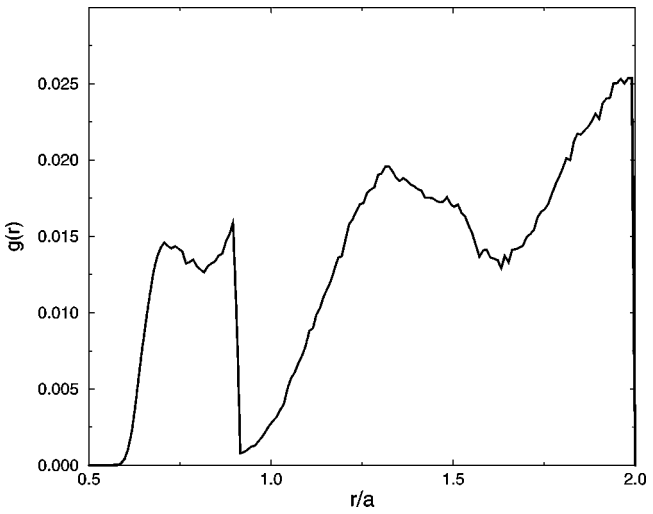


FIG. 10. Radial distribution function *between* defects of coordination $c=13$ at $T=0.79$.

Finally, we emphasize that our results were obtained with simulations using a combination of local and volume updates. However, the use of only collective updates with variable volume as in our previous work[10] does not alter our conclusion, though the equilibrating time is somewhat longer.

## IV. CONCLUDING REMARKS

We have studied the melting mechanism of a fcc solid with the LJ potential. The results show that defects created in the solid phase become numerous enough to cause the crystal to melt. At the transition, about one fourth of the total sites do not have the coordination number 12 of the perfect structure. Just above the transition, only about 20% have 12 NN. Our analysis of the structure of defects shows that a defect is surrounded by atoms at $r$ about $\sqrt{2}/2$ (NN distance) and by atoms at $r$ about $\sqrt{3}/2$ which is not the NNN distance $(=1)$ of the perfect structure. A closer examination shows that these atoms are themselves defects created by dislocating atoms to somewhere between NN and NNN distances. These dislocated positions correspond to ''bridge'' positions in the potential landscape. We note that statistics taken between defects shown above indicate that defects are linked together at the transition. In other words, the assumption of linear defects by Burakowsky, Prestoni, and Silbar[12] is somewhat verified here. By linear defects, one should understand ''strings'' of defects which are not necessarily straight lines of defects. Of course, other aspects of their theory should be further checked, but this is out of the scope of the present work.

## ACKNOWLEDGMENTS

We are grateful to E. Jagla for useful discussions. L.G. and A.D. thank the University of Cergy-Pontoise for hospitality. Laboratoire de Physique Théorique et Modélisation is associated with CNRS (ESA 8089).

[1] N. W. Aschrof and N. D. Mermin, *Solid State Physics* (Saunders, Philadelphia, 1976).
[2] F.A. Linderman, Phys. Z **11**, 609 (1910).
[3] N.D. Mermin, Phys. Rev. Lett. **176**, 250 (1968).
[4] D.R. Nelson and B.I. Halperin, Phys. Rev. B **19**, 2457 (1979).
[5] J.M. Kosterlitz and D.J. Thouless, J. Phys. C **6**, 1181 (1973).
[6] J.M. Kosterlitz, J. Phys. C **7**, 1046 (1974).
[7] H. Kleinert, *Gauge Fields in Condensed Matter* (World Scientific, Singapore, 1989), Vol. II.
[8] B.E. Clements and D.C. Wallace, Phys. Rev. E **59**, 2955 (1999).
[9] W. Brostow, M. Chybicki, R. Laskowski, and J. Rybicki, Phys. Rev. B **57**, 13 448 (1998).
[10] L. Gómez, A. Dobry, and H.T. Diep, Phys. Rev. B **55**, 6265 (1997).
[11] M.I. Katsnelson and A.V. Trefilov, cond-mat/9906402 (unpublished).
[12] L. Burakovsky, D. Preston, and R.R. Silbar, Phys. Rev. B **61**, 15 011 (2000).
[13] M. Kleman and J.F. Sadoc, J. Phys. (France) Lett. **40**, L569 (1979).
[14] L. Gómez and H.T. Diep, Phys. Rev. Lett. **10**, 1807 (1995).
[15] M. P. Allen and D. J. Tildesley, *Computer Simulation of Liquids* (Oxford University Press, Oxford, 1987).
[16] D.K. Chokappa, S.J. Cook, and P. Clancy, Phys. Rev. B **39**, 10 075 (1989).
[17] S.R. Phillpot, J.F. Lutsko, D. Wolf, and S. Yip, Phys. Rev. B **40**, 2831 (1989); J.F. Lutsko, D. Wolf, S.R. Phillpot, and S. Yip, *ibid.* **40**, 2841 (1989).
[18] P. Richard, A. Gervois, L. Oger, and J.-P. Troadec, Europhys. Lett. **48**, 415 (1999).